INTERNATIONAL ATOMIC ENERGY AGENCY
UNITED NATIONS EDUCATIONAL, SCIENTIFIC AND CULTURAL ORGANIZATION

INTERNATIONAL CENTRE FOR THEORETICAL PHYSICS
34100 TRIESTE (ITALY) - P.O.B. 586 - MIRAMARE - STRADA COSTIERA 11 - TELEPHONE: 2240-1
CABLE: CENTRATOM - TELEX 460392 - I

H4.SMR/285 - 20

WINTER COLLEGE ON
LASER PHYSICS: SEMICONDUCTOR LASERS
AND INTEGRATED OPTICS

(22 February - 11 March 1988)

SPATIAL AND TEMPORAL INSTABILITIES IN MULTISTRIPE SEMICONDUCTOR LASERS

T.E. ROZZI
Universita degli Studi di Ancona
Ancona, Italy

Spatial and temporal instabilities in multistripe semiconductor lasers

T. E. Rozzi and K. A. Shore

School of Electrical Engineering, University of Bath, Claverton Down, Bath BA2 7AY, England

Received July 25, 1984; accepted September 24, 1984

We review techniques for the analysis of spatial and temporal instabilities in laser devices. The spatial problem and the temporal problem are first considered in isolation. We then proceed to study their interaction, which requires the development of a novel approach based on the Hopf bifurcation theory. This analysis highlights a number of controllable instabilities effects that can be exploited in optical switching and logic applications.

1. INTRODUCTION

A discussion of spatial and temporal instabilities in semiconductor lasers may be initiated by two contrasting objectives. On the one hand, optical communications systems have a requirement of stable optical sources. In the case of high-bit-rate optical communications, this implies a need for mode-stabilized semiconductor lasers. Hence every effort is made to eliminate the causes of spatial, temporal, and spectral instability in lasers designed for such applications. However, in seeking to apply the semiconductor laser in the role of a high-speed optical switch or as an optical logic element, means are sought to utilize controllable instabilities in the device. To date, the emphasis in research has been on achieving stable lasers, but greater attention is now being given to the development of lasers for switching and logic functions. The design of such devices requires a description of the stability properties of the laser in which both spatial and temporal aspects need to be considered. Techniques of analysis that address this problem are the subject of this paper.

We attempt to review the development of our work, which was initially directed at characterizing spatial stability in conventional single-stripe semiconductor lasers but which led to a framework for stability analysis in which the detailed behavior of the device was taken into account. Insights gained in the theoretical treatment of these problems showed that multistripe devices were prominent candidates for devices exhibiting controllable instabilities. Attention has thus been directed at examining the utilization of these multistripe lasers in which both electronic and optical means of stability control are available. The full potential of these devices, it is believed, is yet to be realized. In discussing these aspects, we include the essentials of the analysis at each stage and summarize the main results obtained in respect of spatial and temporal stability. The exploitation of these results for switching and logic purposes is noted where appropriate.

The organization of the paper follows the logic of the theoretical developments. Thus Section 2 considers the characterization of spatial instability by means of a definition of an instability index. Section 3 shows how controlled spatial instability may be effected. In Section 4, an analysis of high-speed transverse mode switching in the laser is given. The problem of temporal instability is introduced in Sections 5 and 6 on the basis of the classical small-signal analysis. The above approach is restrictive in the case of interplay between temporal and spatial instabilities. This problem is addressed in Section 7, in which a new formalism better suited to this situation is introduced on the basis of the Hopf bifurcation theory.

2. SPATIAL INSTABILITIES

A. Nonlinearities and Near-Field Shifts

Gain-guided stripe-geometry injection lasers commonly exhibit nonlinearities in their above-threshold light-current characteristics. It is found that the optical near field moves laterally across the output mirror facet as the nonlinear portion of the device's light-current characteristic is encountered. In this process, the near field is displaced from an initially symmetric configuration, with displacements of up to 1 μm being typical. Over a range of injection currents, the asymmetry of the near field increases with current, but, for yet higher injection currents, a sudden snapback to a symmetric field occurs.[1]

Instabilities of the near field of this kind would result in significant changes in coupling efficiency in a laser-fiber optical communications system. It is thus essential, for such an application, to stabilize the near field. This may be achieved by ensuring that real index guiding is provided in the device structure, thus preventing near-field shifts. However, as is discussed below, it is also possible to consider a number of applications that exploit the observed nonlinearities and field instabilities. In this context, the requirement is for means of enhancing the nonlinearities. From either viewpoint, it is of importance to be able to quantify the stability/instability of the device's optical near field. This may be accomplished by means of an *instability index*, the derivation of which is discussed in the Subsection 2.B.

Before the discussion of the instability index, we wish to recall briefly the basic physical processes that underlie the analysis. It should be appreciated that two mechanisms are responsible for guiding the optical field in an active device such as the injection laser. The mechanisms may be represented in the real and imaginary parts of a complex dielectric

0740-3224/85/010237-13$02.00

constant and are commonly referred to as *gain guiding* and *refractive-index antiguiding*. To see the relationship between these mechanisms, we note that the change $\Delta\epsilon$ of the dielectric constant that is due to variation in carrier concentration is given by

$$\Delta\epsilon = (-\rho + j)\frac{gn_0}{2k_0V}. \tag{1}$$

Here, g is the local gain, which is conventionally assumed to be linearly related to the carrier concentration; k_0 is the free-space wave vector; $v = c/n_0$ is the velocity of light in the laser material; and n_0 is the background refractive index.

The parameter of greatest interest in the present discussion is the antiguiding parameter ρ, which measures the relative strengths of changes in the real and imaginary parts of the dielectric constant. The parameter ρ is a positive quantity whose value has been assumed to lie variously between about 0.5 and 6.0. It is clear from Eq. (1) that an increase in g by an increase in the carrier concentration will imply a decrease in the real part of the dielectric constant. This will thus have a refractive-index antiguiding effect since the refractive index is reduced. Conversely, the imaginary part of the dielectric constant is increased with carrier concentration; this then is the gain-guiding mechanism. It is the competition between the two guiding mechanisms that is the cause of the near-field instability under consideration.

In seeking to define an instability index appropriate to the injection laser, an argument is developed on the basis that the optical field in the device seeks a spatially stable position consistent with the gain-guiding and antiguiding mechanisms acting on it. Because of the nonlinearity of the interaction between the optical field and the carrier concentration occurring in the device, the spatially stable position need not correspond to a symmetric optical field. The interaction between the optical field and the carrier concentration is modeled using appropriate carrier concentration and wave equations, and the definition of the instability index proceeds by characterizing spatially stable solutions of these device equations. The actual analysis follows a small perturbation of the system through the device equations and seeks a condition for the convergence of the series solution that arises because of the cumulative effect of the iterative procedure inherent in a self-consistent solution of the device equations.

B. Perturbation Analysis and Instability Index

The cross-sectional geometry of a typical stripe-geometry laser is shown in Fig. 1, in which the coordinate axes are also defined. The mechanisms available for guiding the optical field in the transverse x direction are those discussed in Subsection 2.A. We assume that, because of material changes in the y direction, the optical field is confined by a real index guide. In the device, the active region has a thickness d and a width defined by the finite stripe-contact width a to which current injection into the active region is arranged.

The appropriate device-modeling equations for variations in the x direction are (1) the carrier-diffusion equation

$$D\frac{d^2N_0}{dx^2} + \frac{J}{ed} - BN_0^2 = g_tP_0(x) \tag{2}$$

and (2) the appropriate form of the wave equation

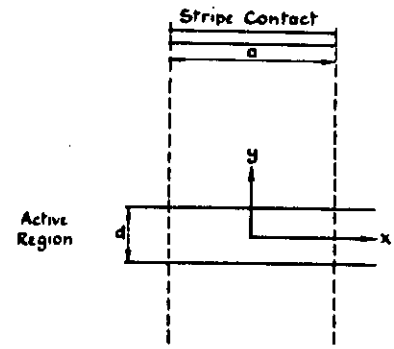

Fig. 1. Schematic cross section for a stripe-geometry laser.

$$\frac{d^2\phi_0}{dx^2} + (\epsilon_0k_0^2 - \beta_0^2)\phi_0 = 0. \tag{3}$$

The terms appearing in the equations are as follows: D is the diffusion coefficient, $N_0(x)$ is the carrier (electron) concentration, J is the injection current, B is the bimolecular recombination coefficient appropriate to low-doped devices, $g_t = \alpha N_0 - \beta$ is the local gain, and $P_0(x) = A_0^2|\phi_0(x)|^2$ is the optical field intensity. A_0 is the field amplitude, and ϕ_0 is the modal field; ϵ_0 is the complex dielectric constant, and β_0 is the longitudinal propagation constant.

The subscript zero appearing on the above quantities denotes the fact that these quantities represent the solutions to the device equations whose stability is to be analyzed. The interaction between the equations is apparent since ϕ_0 from Eq. (3) appears explicitly in Eq. (2), and also N_0 from Eq. (2) appears in ϵ_0 in Eq. (3) by the relationship given in Eq. (1).

The field normalization is written as

$$\int_{-\infty}^{\infty}\phi_0^2(x)dx = 1. \tag{4}$$

The photon density is defined as

$$S_0 = A_0^2\int_{-\infty}^{\infty}|\phi_0|^2dx = \int_{-\infty}^{\infty}|\Phi_0|^2dx, \tag{5}$$

where Φ_0 is the total unperturbed field and ϕ_0 is the modal field.

To examine the stability of the above system, a small perturbation is assumed in the injection current, and the consequences for the optical field and carrier density are found.

In response to the small perturbation δj in the current, a perturbation ϕ arises in the optical field, the dielectric constant is perturbed by an amount η, the longitudinal propagation constant is changed by an amount b, and the carrier concentration changes by an amount n. The interrelation among these quantities must now be defined.

The field perturbation is written to first order as

$$\phi = a_0\phi_0 + a_1\phi_1, \tag{6}$$

where ϕ_1 is zero outside the stripe and orthogonal to ϕ_0:

$$\phi_1 \propto \left(\frac{2}{a}\right)^{1/2}\sin\frac{2\pi x}{a} - \left[\int_{-a/2}^{+a/2}\left(\frac{2}{a}\right)^{1/2}\sin\frac{2\pi x}{a}\phi_0dx\right]\phi_0 : |x| \leq \frac{a}{2}$$

$$\int_{-\infty}^{+\infty}\phi_1^2dx = 1.$$

The wave equation (3) becomes to first order

$$\frac{d^2\phi}{dx^2} + (\epsilon_0 k_0^2 - \beta_0^2)\phi = (2\beta_0 b - \eta k_0^2)A_0\phi_0. \tag{7}$$

By utilizing Eq. (6), it is then possible to calculate

$$a_1 = \frac{k_0^2 A_0 \eta_{01}}{(\beta_0^2 - \beta_1^2)}, \tag{8}$$

where

$$\eta_{01} = \int_{-\infty}^{\infty} \phi_0 \eta \phi_1 dx \tag{9}$$

and

$$\beta_1^2 = k_0^2 \frac{2}{a} \int_{-a/2}^{a/2} \phi_1 \epsilon_0 \sin^2 \frac{2\pi x}{a} dx - \left(\frac{2\pi}{a}\right)^2. \tag{10}$$

Then, from Eq. (1), we may relate η to n, the perturbation in the carrier concentration, and hence rewrite Eq. (8) in the form

$$a_1 = \frac{A_0(-\rho + j)\alpha\omega n_{01}}{(\beta_0^2 - \beta_1^2)V^2}, \tag{11}$$

where n_{01} is the matrix element of n with ϕ_0 and ϕ_1.

We now consider the perturbed form of Eq. (2) again, retaining only first-order terms. We obtain

$$\frac{2n}{\tau_s} + \alpha n P_0 = \frac{\delta j}{ed} - g_0 p(x). \tag{12}$$

The recombination term of the first-order equation is written in terms of an electron lifetime

$$\tau_s = 1/BN_0. \tag{13}$$

The additional diffusion term associated with the perturbation n is neglected in Eq. (12).

The perturbation field intensity $p(x)$ has been introduced into Eq. (12). By definition,

$$p(x) = \phi\Phi_0^* + \phi^*\Phi_0, \tag{14}$$

and, to first order, we have

$$p(x) = A_0[2a_0|\phi_0|^2 + 2\,\mathrm{Re}(a_1\phi_1\phi_0^*)]. \tag{15}$$

An iterative procedure is now followed between Eqs. (11) and (12) and utilizing Eq. (15). For the first cycle of the iteration, we take $p(x) = 0$, so that, from Eq. (12),

$$n = n^{(1)} = \frac{\tau_s \delta j}{2 + \alpha\tau_s P_0}. \tag{16}$$

Equation (16) may be used in Eq. (11) to find

$$a_1^{(1)} = \frac{A_0}{(\beta_0^2 - \beta_1^2)}(-\rho + j)\frac{\alpha\omega\tau_s}{V^2}\int_{-\infty}^{\infty} \frac{\phi_0 \delta j \phi_1}{2 + \alpha\tau_s P_0} dx. \tag{17}$$

The second cycle of the iteration takes $p(x)$ into account, so that

$$n = n^{(1)} + n^{(2)} = n^{(1)} - \frac{g_0\tau_s}{2 + \alpha\tau_s P_0} p(x). \tag{18}$$

In writing $a_1 = a_1^{(1)} + a_1^{(2)}$ from Eqs. (18), (15), and (11), we find an expression for $a_1^{(2)}$. This process may be continued through further iterations. The repetition of the procedure thus provides series expansions for the perturbations a_1 and n as infinite sums. It is possible to show that the convergence of these sums is determined, in cases of physical interest, by the ratio

$$R = \left|\frac{a_1^{(2)}}{a_1^{(1)}}\right|. \tag{19}$$

For $R < 1$, the series for a_1 is convergent. This then implies that the optical field develops a finite perturbation $a_1\phi_1$ and is thus stable. When $R > 1$, the perturbation to Φ_0 is no longer finite, and so it is the case that the initial state is unstable. So R may be used to define the stability of the optical field and is thus called the *instability index* of the mode.

Under certain approximations, it is found that the instability index may be written as

$$R = \left| 2A_0 \frac{\int_{-\infty}^{\infty} \phi_0\,\mathrm{Re}[a_1^{(1)}\nu]\phi_1 dx}{\int_{-\infty}^{\infty} \frac{\phi_0\tau_s\delta j\phi_1}{2 + \alpha\tau_s P_0} dx} \right|, \tag{20}$$

where

$$\nu(x) = \frac{g_0\tau_s}{2 + \alpha\tau_s P_0}\phi_1\phi_0^*. \tag{21}$$

It is pointed out that Eqs. (17) and (20) imply that R is, in fact, independent of the perturbation δj.

Application of the foregoing definition of the instability index to calculations of the properties of a typical stripe-geometry laser demonstrated that the index correctly described the nonlinear behavior of the device.[2] The calculations followed the instability index along the light-current characteristics of the device. It was found that

1. For relatively low injection currents, the light-current characteristics were linear, the near field was symmetric, and the instability index was small, i.e., less than about 0.5.
2. As the injection current was increased to a nonlinear portion of the light-current characteristic, the instability index rapidly increased (in fact, assuming values greater than unity), but the near field remained symmetric.
3. Further increase in the current resulted in a shift of the near field to an asymmetric off-center position and also a decrease in the instability index to a value of about 0.5.
4. Yet further increases in the current saw an increase in the stability index for an asymmetric near field and then a snapback to a symmetric near field, at which point the stability index again fell to values of 0.5 or less.

The interpretation of these findings is that, in case 2, the near field occupied an unstable symmetric configuration and, with a suitable perturbation of the injection current, then moved into the stable asymmetric configuration of case 3. The existence of this stable off-center configuration will form the basis of a theory of transverse mode switching that is developed below. The results in case 4 indicate that the asymmetric configuration itself becomes unstable, and the field once again seeks a stable configuration that is a symmetric configuration associated with hole burning in the local gain. The effect of the hole burning, which occurs for comparatively high optical output powers, is to produce an index-guiding effect in the device that favors a symmetric near field.

Inasmuch as the conclusions of the stability analysis using the instability index R are both internally consistent with calculated optical field profiles and also agree qualitatively with experimental results, it is claimed that this approach is a valid method of assessing nonlinearities in the device characteristics. With this basis for analyzing the stability of transverse modes, our attention now turns to seeking ways of exploiting the nonlinearities in the laser. As noted above, one particularly interesting consequence of the stability analysis is the possibility of transverse mode switching between stable asymmetric states. The description of these effects requires a consideration of time-dependent diffusions and wave equations and is discussed further in Section 4. In Section 3, we consider methods of exploiting controlled instabilities under static conditions.

3. CONTROLLED INSTABILITY AND ITS APPLICATIONS

A. Electronically Controlled Instability

The foregoing analysis of spatial instability that may arise in conventional stripe-geometry lasers showed how the optical near field could undergo a spatial translation under appropriate conditions. In single-stripe devices, this behavior is determined, by the complex dielectric constant, by the form of the local gain function. Gain guiding, which confines the optical field over a range of the light-current characteristics, may give way to real-index guiding for higher optical powers when the injection current is significantly increased. The fundamental difficulty, however, is that little control can be effected over the form of the gain function in single-stripe devices. This is unfortunate, since the near-field shifts and nonlinearities that appear in stripe-geometry lasers are potentially useful. The position may be recovered by the rather simple expedient of constructing multistripe-geometry lasers and, in particular, twin-stripe lasers. In such devices, it is found that control can be exercised over the optical near field by means of independently controllable injection currents. The extra degree of freedom introduced by applying a second stripe contact to the device is sufficient to transform the laser into a useful component in a number of applications. Such electronic means of controlling near-field instability in the laser are discussed below. In Subsection 3.B, it is shown how optical injection may be used further to enhance the usefulness of the twin-stripe laser and hence of multistripe lasers.

A schematic cross section of the twin-stripe laser is given in Fig. 2. The active region of the laser is now pumped by two injection currents. It is assumed that electrical isolation between the stripe contacts can be ensured so that the currents J_1 and J_2 may be varied independently. An analysis of this device has been performed using a general model for semiconductor lasers.[3] The essential requirement for carrying out the computer modeling of this device is the ability to include a current profile $J(x)$ that takes account of the currents J_1 and J_2. In all other respects, the solution of Eqs. (2) and (3) for twin-stripe devices is similar to the procedure followed for single-stripe devices.[4] An alternative procedure for analyzing these devices has been suggested by Katz.[5]

Computer analysis of a number of aspects of the behavior of twin-stripe devices has been performed. Here, we highlight

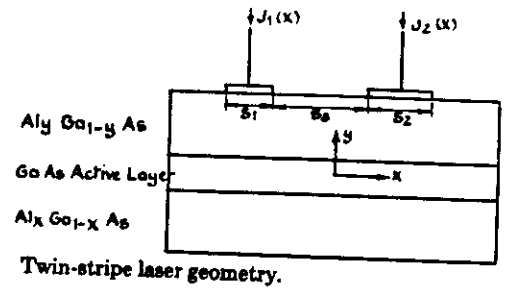

Fig. 2. Twin-stripe laser geometry.

the main conclusions drawn from those computations. Confirmation was obtained of the basic contention that controlled movement of the optical near field could be demonstrated through variation of the injection currents. It is further shown that nonlinear light-current characteristics were a consequence of the movement of the near field.[3] The physical explanation of the latter effect is quite straightforward. It is apparent that the movement of the near field into the unpumped interstripe region of the active layer will cause the field to experience a reduced gain. The intensity in the near field will thus tend to decrease even though the controlling injection current may be increased in order to bring about near-field movement. It follows from these observations that interstripe coupling processes play an important role in determining the extent to which near-field shifts can be accomplished. The coupling between the stripes is affected by interstripe separation, carrier diffusion, and current-spreading effects.[6] The first of these is most easily adjusted at the device design stage. The degree of electrical isolation between the stripes must be carefully considered to account for current-leakage effects.[7] Finally, reference is made to calculations of the optical output power of the device and a function of the injection currents J_1 and J_2.[8] When the results of these calculations are displayed in the form of constant-power contours in the J_1–J_2 plane, they provide confirmation of measured results that have been developed to show the occurrence of bistability in twin-stripe lasers.[9]

Practical applications of the effects outlined above have been discussed in two main areas. The earliest suggestions for using the twin-stripe laser were with respect to a scanning function, in which controlled movement of the device far-field radiation pattern was of interest.[10] The rotation of the far-field pattern as injection currents are altered may be seen to be a consequence of the near-field shifts already discussed in Refs. 3 and 6. Further remarks on this application will be made in the discussion of optically controlled instability in Subsection 3.B. The second area of interest in which exploitation of twin-stripe laser properties is under active investigation has already been referred to and concerns the use of the device as an optical logic element. Bistability in these devices is well known by now, but there remains work to be done to optimize switching times and other operating parameters to realize useful ultrafast logic devices. It should be remarked for completeness that multistripe devices have received considerable attention recently because of their capability for providing large optical output powers. This aspect will not be pursued here, since the phase-locking properties responsible for this feature of multistripe-device characteristics do not belong to a discussion of optical instability.

B. Optically Controlled Instability

The previous subsection considered the scope offered by the twin-stripe laser in particular and multistripe lasers in general for controlling near- and far-field patterns. The basis for electronic control of the optical field was the change in the gain profile in the device that could be effected by independent adjustment of the stripe currents. It is natural to inquire how the static properties of the device may be influenced by means of the injection of light into the active region of the laser. The superposition of the injected light upon the lasing optical field causes a change in the lateral gain profile, and hence the wave-guiding characteristics of the structure are altered. So that optical injection may have significant effects, it is necessary to be able to adjust the sensitivity of the device, i.e., to choose a gain profile that implies a potentially unstable optical lasing field. Since control of the near-field position is offered by multistripe devices, it is in that context that optical injection effects are assessed.

In Fig. 3, we show a schematic diagram of the twin-stripe laser subject to optical injection into the active region below either or both of the stripe contacts. By taking an incoherent superposition of injected and lasing optical fields and by further assuming that the injected light is at the lasing frequency, a simple modification of the carrier diffusion equation is all that is required to model optical injection effects. We now have

$$D\frac{d^2n}{dx^2}+\frac{J(x)}{ed}=g_t[P(x)+P_{IN}(x)]+Bn^2. \tag{22}$$

Comparison with Eq. (2) reveals that an additional term $gtP_{IN}(x)$ is now included, where $P_{IN}(x)$ represents the injected optical intensity.

A series of calculations was performed to provide estimates of likely effects of optical injection on near-field movement and consequent changes in output characteristics of the device. It was shown how the sensitivity of the device to optical injection could be tuned by the variation in currents J_1 and J_2. Significant changes in the lasing-field intensity were demonstrated for relatively small optical injection powers.[11,12] The latter observation was developed to show optically induced bistable action in the twin-stripe laser.[13] It is believed that the latter effect will be of particular interest in the context of optical logic. As an all-optical approach to implementing bistability, it avoids recourse to electronic means of switching and thus is potentially fast in this response and also lends itself to integration in an all-optical circuit.

Two other applications-oriented sets of calculations were made. In the first, it was shown how the effects of near-field instability could be carefully tuned to produce optical limiter action in the device. In this case, the total light output from the device remained constant over a range of injected optical power.[14] Second, the optically driven analog to the beam scanner discussed above was assessed. It was shown that rotation of the far field could indeed be achieved by optical means, and, further, that the required optical injection power was not unreasonable. The calculations indicated that a far-field rotation of between 1° and 3° per milliwatt of injected optical power may be achievable.[15] Although such field rotations are less than what would be expected with electronically steered beam scanners, the ability to perform the scanning by optical means alone may still have attractions.

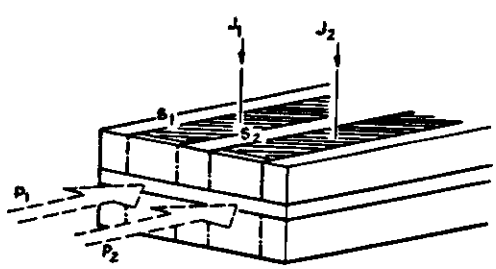

Fig. 3. Optical injection into a twin-stripe laser.

In this section, attention has been paid to the manner in which spatial instability may be exploited to develop the static properties of the semiconductor laser. In Section 4, we turn to the effects of spatial instabilities on the dynamical properties of the laser.

4. TRANSVERSE MODE SWITCHING

As was discussed in Section 2, nonlinearities in light-current characteristics of single-stripe-geometry lasers may be associated with the appearance of off-center optical fields even in an apparently symmetric device. In an ideal laser, such asymmetric near fields are degenerate; two asymmetric off-center positions for the field are possible, one being the mirror image of the other. In practice, there may be nonuniformities in the device that serve to break the degeneracy and hence determine that only one of the positions is tenable. Nevertheless, it is of interest to consider the ideal case in which two asymmetric situations are allowed. In this case, there is no *a priori* reason to choose between a field that is off-center to the right and a field that is off center to the left. Since either position may occur, it may then be possible to establish oscillations between the two off-center states. The point of interest is the frequency of such oscillations, and we will not be concerned at this point about the conditions that must obtain in order to establish such oscillatory behavior. This aspect will be addressed in the discussion of the Hopf algorithm given in Section 7. We give here a derivation of the oscillation frequency for a particular class of oscillations that may be established between the degenerate states under consideration. The class of oscillations is characterized by the constraint that the power in the oscillating field be a constant. The formalism includes the possibility of fluctuations in the optical power, but that aspect is not developed.

To proceed with the analysis, it is assumed that solutions to the steady-state diffusion and wave equations [Eqs. (2) and (3)] are found such that an asymmetric modal field $\phi_a(x)$ is obtained with a corresponding carrier distribution $N_a(x)$. Under the postulate of degeneracy of the solution, a second steady solution is possible, for which

$$\phi_b(x)=\phi_a(-x) \tag{23}$$

and

$$N_b(x)=N_a(-x). \tag{24}$$

A time-varying optical field is then taken to be

$$\phi(x,t)=a(t)\phi_a(x)+b(t)\phi_b(x). \tag{25}$$

In general, ϕ would satisfy the time-dependent wave equation

$$\nabla^2\phi - \frac{\epsilon}{c^2}\frac{\partial^2\phi}{\partial t^2} = \frac{2}{c^2}\frac{\partial\phi}{\partial t}\frac{\partial\epsilon}{\partial t} + \frac{1}{c^2}\phi\frac{\partial^2\epsilon}{\partial t^2}. \tag{26}$$

We separate the time variation into two components, one of which is related to the optical-carrier frequency ω_0, the other being due to the slow variations of the field amplitudes:

$$\frac{\partial}{\partial t} = j\omega_0 + \frac{\partial}{\partial\tau}. \tag{27}$$

Then the wave equation becomes

$$\nabla^2\phi + \frac{\omega^2}{c^2}\epsilon\phi = \frac{2j\omega_0}{c^2}\epsilon\left(\frac{\partial\phi}{\partial\tau} + \frac{1}{\epsilon}\frac{\partial\epsilon}{\partial\tau}\phi\right). \tag{28}$$

By definition,

$$\nabla^2\phi_a + n_a{}^2k_0{}^2\phi_a = 0, \tag{29}$$

$$\nabla^2\phi_b + n_b{}^2k_0{}^2\phi_b = 0. \tag{30}$$

Hence the wave equation reduces to

$$ak_0{}^2(n^2 - n_a{}^2)\phi_a + bk_0{}^2(n^2 - n_b{}^2)\phi_b = \frac{2j\omega_0}{c^2}n^2\left(\frac{\partial\phi}{\partial\tau} + \frac{1}{n^2}\frac{\partial n^2}{\partial\tau}\right), \tag{31}$$

where $\epsilon(t) = n^2(t)$.

The stationary carrier distributions satisfy the equations

$$D\frac{\partial^2N_a}{\partial x^2} + \frac{J(x)}{ed} - \frac{N_a(x)}{\tau_a} - g_{ta}S_0|\phi_a(x)|^2 = 0, \tag{32}$$

$$D\frac{\partial^2N_b}{\partial x^2} + \frac{J(x)}{ed} - \frac{N_b(x)}{\tau_b} - g_{tb}S_0|\phi_b(x)|^2 = 0. \tag{33}$$

S_0 appears in both equations because of the degeneracy assumption. Note that electron lifetimes τ_a and τ_b have been used instead of the bimolecular term involving B that appears in Eq. (2).

The time-dependent diffusion equation satisfied by the carrier density is

$$\frac{\partial N(x,t)}{\partial t} = \frac{\partial N}{\partial\tau} = \frac{J(x,t)}{ed} - \frac{N(x,t)}{\tau_s} + D\frac{\partial^2N}{\partial x^2} - g_tP(x,t). \tag{34}$$

We introduce variations from the stationary states as

$$\tilde{N}_a(x,t) = N(x,t) - N_a(x), \tag{35}$$

$$\tilde{N}_b(x,t) = N(x,t) - N_b(x), \tag{36}$$

and it is found that these quantities satisfy the equations

$$\frac{\partial\tilde{N}_a}{\partial\tau} + \frac{\tilde{N}_a}{\tau_s} + \alpha_t\tilde{N}_aP_a = -g_{ta}(P - P_a), \tag{37}$$

$$\frac{\partial\tilde{N}_b}{\partial\tau} + \frac{\tilde{N}_b}{\tau_s} + \alpha_t\tilde{N}_bP_b = -g_{tb}(P - P_b), \tag{38}$$

where $P_a = S_0|\phi_a(x)|^2$, $P_b = S_0|\phi_b(x)|^2$, and $g_t = \alpha_tN - \beta_t$.

Making use of Eq. (1) once again, we may deduce that

$$n^2 - n_a{}^2 = (-\rho + j)\frac{\alpha_tn_0}{Vk_0}\tilde{N}_a, \tag{39}$$

$$n^2 - n_b{}^2 = (-\rho + j)\frac{\alpha_tn_0}{Vk_0}\tilde{N}_b. \tag{40}$$

Equations (31), (37), and (38) must now be solved for the optical field ϕ. To identify the frequency of oscillation, we assume that

$$a(t) = (S_0)^{1/2}(a_0 + a_1\cos\omega t), \tag{41}$$

$$b(t) = (S_0)^{1/2}jb_1\sin\omega t. \tag{42}$$

Then

$$S(t) = |a(t)|^2 + |b(t)|^2 = \left(a_0 + \frac{a_1{}^2 + b_1{}^2}{2} + 2a_0a_1\cos\omega t + \frac{a_1{}^2 - b_1{}^2}{2}\cos 2\omega t\right). \tag{43}$$

To meet the constraint that $S(t) = \text{constant} = S_0$, it follows that either $a_0 = 1$ and $a_1 = b_1 = 0$ or $a_0 = 0$ and $a_1 = b_1 = 1$. The second choice represents the required oscillation between states a and b.

Thus we have

$$da/d\tau = j\omega b, \tag{44}$$

$$db/d\tau = j\omega a. \tag{45}$$

These postulates lead to a definition of the oscillation frequency ω.[16] The detailed derivation utilizes a Fourier expansion of the type

$$\tilde{N}_a(x,t) = n_0{}^a(x) + n_{1c}{}^a(x)\cos\omega t + n_{1s}{}^a\sin\omega t + \ldots.$$

We can deduce that

$$n_0{}^a = \frac{g_{ta}}{2}S_0\frac{(|\phi_a|^2 - |\phi_b|^2)}{(1/\tau_s + \alpha_tP_a)} \tag{46}$$

and

$$n_{1c}{}^a = n_{1s}{}^a = 0. \tag{47}$$

Finally, it is shown that

$$\frac{\omega}{\omega_0} = (-\rho + j)\frac{\alpha_t}{2n_0k_0V}\int_{-\infty}^{\infty}\phi_b{}^*n_0{}^a\phi_a\,dx \tag{48}$$

(an equivalent expression involving $n_0{}^b$ is also found).

The calculated oscillation frequency ω will be a complex quantity, and, hence, real oscillations can arise only at isolated points at most, and then the real part of ω can be taken as the oscillation frequency. Numerical calculation of Eq. (48), using typical parameters for the device, indicated oscillation frequencies varying between 10 and 150 GHz,[17] thus implying optical switching times in the range of a few nanoseconds down to a few picoseconds.[18] Hence the generation of such oscillations would be of considerable interest in the context of high-speed optical switches. It is emphasized that the oscillations are of a particular kind, in which the total optical power is a constant. As was found in the discussion following Eq. (43), two possibilities exist within the formalism to meet the constraint of fixed optical power. The first possibility was defined by $a_0 = 1$ and $a_1 = b_1 = 0$, i.e., a steady-state solution. The derivation outlined above concerned the oscillating behavior defined by $a_0 = 0$ and $a_1 = b_1 = 1$. The question arises whether a transition can occur between these two kinds of solution. This problem has been approached within the context of Hopf bifurcation theory and is discussed in Section 7. As a final reference to Eq. (43), we point out that it allows also for a fluctuation in the total photon density at frequency

ω, 2ω, or a combination of such fluctuations with a constant-background photon intensity. We will now turn to the question of describing the general dynamic behavior of the laser on the basis of a basic spatial model.

5. TEMPORAL INSTABILITY

We consider the following system of rate equations describing the time evolution of a laser mode feeding on the inversion of two reservoirs. These reservoirs can be two transverse or longitudinal regions, two spatial Fourier components of the carrier density distribution, two different types of recombination mechanism, etc. We include the effect of saturable absorption as well as of diffusion coupling at first without spontaneous emission:

$$\frac{dS}{dt} = \left(G - \frac{1}{\tau_p}\right) S, \tag{49a}$$

$$\frac{dN_1}{dt} = -\frac{N_1}{\tau_{s(1)}} + j_1 - C_1 S g_1(N_1) + \frac{N_2 - N_1}{\tau}, \tag{49b}$$

$$\frac{dN_2}{dt} = -\frac{N_2}{\tau_{s(2)}} + j_2 - C_2 S g_2(N_2) + \frac{N_1 - N_2}{\tau}, \tag{49c}$$

where S is the photon density. N_1 and N_2 are the carrier densities in reservoirs 1 and 2, respectively, with lifetimes $\tau_{s(1,2)}$. τ_p is the photon lifetime, and τ is the diffusion time constant. $g_i(N_i)$ is the gain function in reservoir 1. The gain functions in the two reservoirs are taken as different in general, allowing for the possibility of inhomogeneities. The optical gain G is given by

$$G = C_1 g_1(N_1) + C_2 g_2(N_2), \tag{50a}$$

where the coefficients C_1 and C_2 describe the distribution of optical power between the two reservoirs and are such that

$$C_1 + C_2 = 1. \tag{50b}$$

j_i are the nominal current densities in units of the electron charge.

A stationary solution of the above equations is obtained when the time derivatives are zero:

$$C_1 g_1(N_1) + C_2 g_2(N_2) = \frac{1}{\tau_p}, \tag{51a}$$

$$N_1\left[\frac{1}{\tau_{s(1)}} - \frac{1}{\tau}\right] - \frac{N_2}{\tau} + C_1 S g_1(N_1) = j_1, \tag{51b}$$

$$\frac{-N_1}{\tau} + N_2\left[\frac{1}{\tau_{s(2)}} + \frac{1}{\tau}\right] + C_2 S g_2(N_2) = j_2. \tag{51c}$$

Eliminating N_1 and N_2 from these equations, we obtain a curve

$$S = S(j_1, j_2). \tag{51d}$$

It is obvious from the rate equations that the solution $S = 0$ is stable below threshold. Instability can arise only for $S > 0$, however small S may be.

In order to investigate the stability conditions of the above system, we linearize the above rate equations around the stationary points S, N_1, and N_2 so that

$$S(t) = S + s(t),$$
$$N_i(t) = N_i + n_i(t). \tag{52}$$

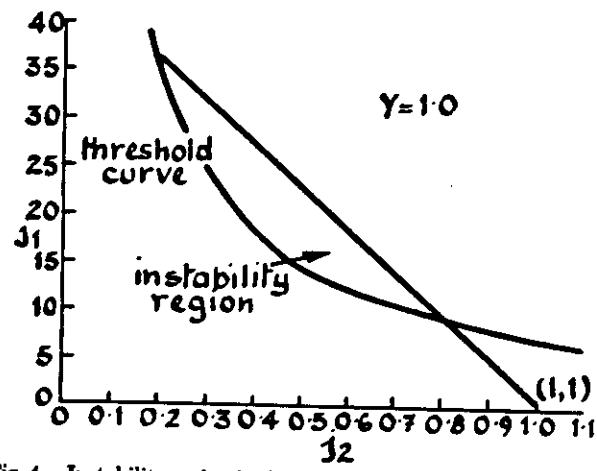

Fig. 4. Instability region in the J_1–J_2 plane.

This yields

$$\frac{ds}{dt} = \left(C_1 \frac{\partial g_1}{\partial n_1} n_1 + C_2 \frac{\partial g_2}{\partial n_2} n_2\right) S, \tag{53a}$$

$$\frac{dn_1}{dt} = -\frac{n_1}{\tau_1} + \frac{n_2}{\tau} - C_1 s g_1(N_1), \tag{53b}$$

$$\frac{dn_2}{dt} = \frac{n_1}{\tau} - \frac{n_2}{\tau_2} - C_2 s g_2(N_2), \tag{53c}$$

where

$$\frac{1}{\tau_i} = \frac{1}{\tau_{s(i)}} + \frac{1}{\tau} + C_i S \frac{\partial g_i}{\partial n_i} \tag{54}$$

and the derivatives are taken at the equilibrium point. According to the Hurwitz criterion,[19] the linearized equations above yield stable solutions under the following conditions:

$$\left(\frac{1}{\tau_1} + \frac{1}{\tau_2}\right)\left(\frac{1}{\tau_1 \tau_2} - \frac{1}{\tau^2}\right) + S\left[C_1 g_1(N_1)\left(C_1 \frac{\partial g_1}{\partial n_1}\frac{1}{\tau_1} - C_2 \frac{\partial g_2}{\partial n_2}\frac{1}{\tau}\right) + C_2 g_2(N_2)\left(C_2 \frac{\partial g_2}{\partial n_2}\frac{1}{\tau_2} - C_1 \frac{\partial g_1}{\partial n_1}\frac{1}{\tau}\right)\right] > 0, \tag{55a}$$

$$g_1(N_1)\left(C_1 \frac{\partial g_1}{\partial n_1}\frac{1}{\tau_2} + C_2 \frac{\partial g_2}{\partial n_2}\frac{1}{\tau}\right) + g_2(N_2)\left(C_1 \frac{\partial g_1}{\partial n_1}\frac{1}{\tau} - C_1 \frac{\partial g_2}{\partial n_2}\frac{1}{\tau_1}\right) > 0. \tag{55b}$$

Additional to these conditions is the criterion discussed under Eq. (51d), namely,

$$S(j_1, j_2) > 0. \tag{55c}$$

If we neglect diffusion coupling in the above conditions, i.e., $(1/\tau) \to 0$, these conditions reduce to Basov's stability criteria:

$$\left(\frac{1}{\tau_1} + \frac{1}{\tau_2}\right)\frac{1}{\tau_1 \tau_2} + S\left[C_1^2 g_1(N_1) C_1 \frac{\partial g_1}{\partial n_1}\frac{1}{\tau_1} - C_2^2 g_2(N_2)\frac{\partial g_2}{\partial n_2}\frac{1}{\tau_2}\right] > 0, \tag{56a}$$

$$C_1 \frac{\partial g_1}{\partial n_1}\frac{g_1}{\tau_2} + C_1 \frac{\partial g_2}{\partial n_2}\frac{g_2}{\tau_1} > 0, \tag{56b}$$

where now

$$\frac{1}{\tau_1} = \frac{1}{\tau_{si}} + C_i S \frac{\partial g_i}{\partial n_i}. \tag{57}$$

By comparing Eqs. (55a) and (56a), taking into account that the definition of τ_i is different in the two cases, it appears that the effect of diffusion is to reduce the region of potential instability in J_1–J_2 plane. A typical such region in absence of diffusion is shown in Fig. 4.

In the following section, we consider one example of a more refined spatial model, including the effect of spontaneous emission.

6. VARIABLE-SLAB-WAVEGUIDE MODEL

The basic layer cross section is that in Fig. 1. Figure 5 represents an equivalent three-layer slab parallel to the junction. n_i is the effective refractive index of region i, related to the carrier concentration N_i by the relationship

$$n_i = n_0 + (-\mu + j)\frac{n_0}{c}\frac{g_i}{2k_0}, \tag{58}$$

$$g_i = \beta\left(\frac{N_i}{N_0} - 1\right)(s^{-1}), \tag{59}$$

where n_0 is the background's effective refractive index, c is the speed of light *in vacuo*, k_0 is the free-space wave number, μ is the ratio of real and imaginary refractive-index variations with N, g_i is the gain in region i, β is the gain slope, and N_0 is the carrier concentration for transparency. The diffusion equation is modeled by the differential equations

$$\frac{dN_1}{dt} = \frac{j_1}{ed} - \frac{N_1}{\tau_{s1}} + \frac{N_2 - N_1}{\tau_{12}} + c_1 g_1 S, \tag{60a}$$

$$\frac{dN_2}{dt} = \frac{mj_1}{ed} - \frac{N_2}{\tau_{s2}} + \frac{N_1 - N_2}{\tau_{12}} + \frac{N_3 - N_2}{\tau_{23}} - c_2 g_2 S, \tag{60b}$$

$$\frac{dN_3}{dt} = \frac{N_3}{\tau_{s3}} + \frac{N_2 - N_3}{\tau_{23}}, \tag{60c}$$

where $m = j_2/j_1$ is a function of the total injection current, as discussed in Ref. 19, and τ_{si} is the carrier lifetime in region i, which, in the bimolecular model, is given by

$$\tau_{si} = 1/BN_i. \tag{61}$$

τ_{12} is a diffusion-time constant proportional to the product of half-widths of the regions 1 and 2 over the diffusion constant $\tau_{23} \approx \tau_{12}$, S is the photon density, and c_i is the confinement factor in region i, which is a function of the difference $N_1 - N_2$ only:

$$c_1 = c_1(N_1 - N_2) = \frac{\int_0^{a/2} |\phi(x)|^2 dx}{\int_0^{\infty} |\phi(x)|^2 dx}, \tag{62}$$

$$c_1 + c_2 = 1. \tag{63}$$

Within an arbitrary constant, the optical field is given by

$$\phi(x) = \cos\left(u\frac{x}{a/2}\right) : |x| \le a/2$$

$$= \cos u \exp\left[-w\left(\frac{x}{a/2} - 1\right)\right] : |x| \ge a/2. \tag{64}$$

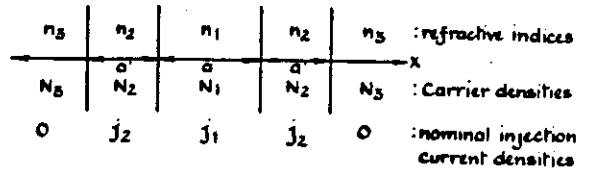

Fig. 5. Equivalent three-layer slab model of laser.

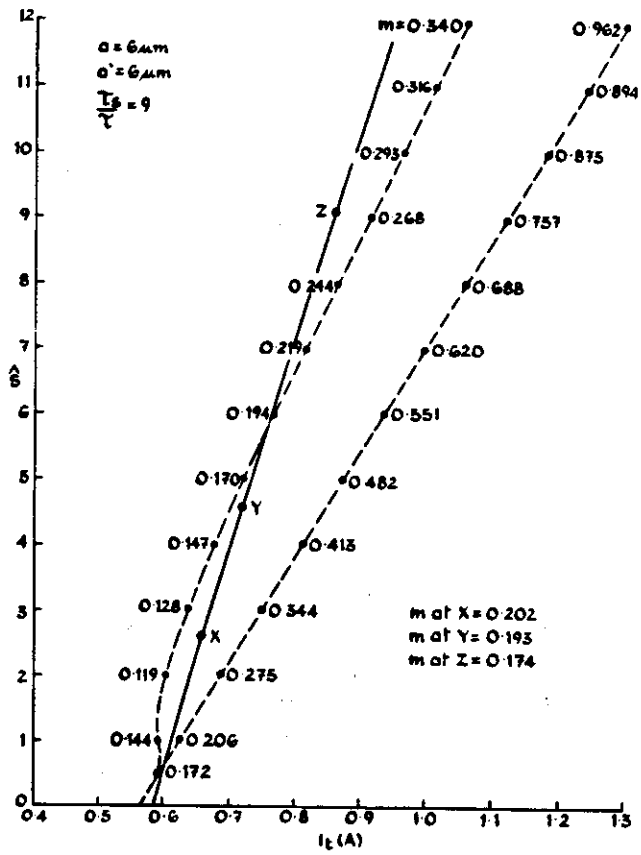

Fig. 6. Instability region in the I_t–S plane.

The normalized wave numbers u and w are the solutions of the dispersion relations $u \tan u = w$:

$$u^2 + w^2 = (n_1^2 - n_2^2)\left(k_0\frac{a}{2}\right)^2$$

$$\approx \frac{a^2}{2} n_0 k_0 (-\mu + j)\frac{n_0\beta}{c}\frac{N_1 - N_2}{N_0}. \tag{65}$$

Here we have neglected a slight difference between the TE and TM modes parallel to the junction. Given a difference of carrier densities, infinite solutions are possible in the complex u plane. We operate in the region where the gain of the fundamental mode only approaches the inverse photon lifetime. Together with Eq. (60), we must consider the optical gain equation

$$\frac{dS}{dt} = \left(G - \frac{1}{\tau_p}\right)S + \xi B(c_1 N_1^2 + c_2 N_2^2)$$

$$\approx \left(c_1 g_1 + c_2 g_2 - \frac{1}{\tau_p}\right)S + \xi B(c_1 N_1^2 + c_2 N_2^2), \tag{66}$$

where $G = 2\beta''(c/n_0)$ is the modal gain, τ_p is the photon lifetime corrected for field confinement in the y direction and

including cavity losses, ζ is the spontaneous-emission constant, and β'' is the imaginary part of the propagation constant:

$$\beta = \left[(n_1 k_0)^2 - \left(\frac{u}{a/2}\right)^2\right]^{1/2} = \left[(n_2 k_0)^2 + \left(\frac{w}{a/2}\right)^2\right]^{1/2},$$

and the approximation in Eq. (66) holds for not-too-narrow stripe widths. The stationary characteristics are obtained by setting the time derivatives equal to zero in Eqs. (60) and (66) and solving for $S = S(J_1, J_2)$ by elimination of N_1, N_2, and N_3.

The stability of the system of first-order differential equations [Eqs. (60)] is investigated by means of the Hurwitz criterion, as outlined in Refs. 19 and 20. This procedure gives the necessary conditions for instabilities. The presence of actual instabilities is checked by checking the formation of limit cycles in the phase space N_1 and N_2.

In deriving the numerical results, we have used in Eqs. (60) the exact expression for the modal gain rather than its approximation. Moreover, the following parameters were kept constant throughout:

$k_0 = 7.48 \times 10^4\ \text{cm}^{-1}$, $\beta = 1.747 \times 10^{12}\ \text{sec}^{-1}$,

$c = 3.0 \times 10^{10}\ \text{cm sec}^{-1}$, $\zeta = 10^{-4}$,

$n_0 = 3.52$, $\tau_p = 2 \times 10^{12}\ \text{sec}$,

$\mu = 3.5$, $\tau_s = 10^{-9}\ \text{sec}$,

$\tau_{12} = \tau_{23} = \tau$, $N_0 = 1.5 \times 10^{18}\ \text{cm}^{-3}$.

Consider first the total injection current I_t as independent variables: Figure 6 illustrates a typical region of instability in the plane $I_t - S$ for a narrow-stripe laser. Also indicated in the figure is the limit value at m within which oscillation takes place.

7. HOPF BIFURCATION METHOD

With a view to exploiting the dynamic behavior of the device, it is necessary to provide means of assessing the stability characteristics in both time and space. The approach to this problem described in the previous sections is to replace the active region by a number of piecewise-uniform subregions, each described by a nonlinear rate equation for the carrier density, perform a small-signal analysis, and apply the Hurwitz criterion to the Laplace transform of the linearized equations.[19]

Inasmuch as the optical field can also be approximately described by the modes of a multilayer slab with stepped refractive-index profile, the above approach also lends itself to an approximate description of the spatial as well as the temporal evolution.[20] One may require, however, to obtain a detailed spatial description by this method or even to describe instabilities in multistripe or split-stripe lasers or more-complicated types of instability in which pulsations are associated with mode changes. Under these more-general conditions, the approach described above becomes rapidly intractable because of the increasing number of coupled rate equations, one per region plus one for the photon density of each mode.

The approach presented in this section goes back to the coupled partial differential equation describing the temporal evolutions and spatial distributions of the carrier and photon densities. The self-consistent steady-state solutions of the two coupled equations are used to define local normal modes, which are time dependent. The temporal and spatial perturbations can then be described as linear combinations of the local normal modes with time-dependent amplitudes. The geometrical interpretation of this process is that of introducing a local system of coordinates along the tangent and the normal at a point of a curve in order to describe small deviations from that point. In this new system of coordinates, the original problem is then reduced to that of analyzing the stability of the rate equations for five scalar amplitudes: the real amplitude of the fundamental optical mode, the amplitude and relative phase of an orthogonal deviation, the real amplitude of the function describing the steady-state electron density, and that of an orthogonal deviation. The classical Hopf bifurcation theory is now applied to the reduced problem in Subsection 7.F. The basic elements of the theory are briefly recalled in Subsection 7.E for ease of reference. Whereas the Hurwitz criterion determines just the regions of potential small-signal instability, the Hopf algorithm provides a means for determining the critical points at which steady-state behavior breaks into two oscillatory solutions (Hopf bifurcation). The existence of a Hopf bifurcation in the characteristics therefore implies the possibility of both bistable operation and self-sustained oscillations. Also, the onset of spatial instability associated with near-field shift and nonlinear light-current characteristics in broad-stripe lasers are easily identified as discontinuities in the eigenvalues of the matrix of the equations of motion.

A. Time-Dependent Wave Equation

From Maxwell's equations, we write the time-dependent wave equations

$$\nabla^2\phi - \mu_0\epsilon\frac{\partial^2\phi}{\partial t^2} = 2\mu_0\frac{\partial\phi}{\partial t}\frac{\partial\epsilon}{\partial t} + \phi\frac{\partial^2\epsilon}{\partial t^2}. \tag{67}$$

The effective-dielectric-constant method is used to reduce the three-dimensional wave equation to two dimensions x and z in the plane of the junction. Propagation is assumed along the z axis, and the origin of the transverse x axis is taken at the midpoint of the device active region. In the case of stripe-geometry lasers, which will be considered in the numerical work below, the origin of x is taken at the stripe midpoint.

It is convenient to separate the time differentials appearing in Eq. (67) into two parts: one corresponding to the optical frequency variation and the other representing variations slow compared with the variation of the optical carrier. Thus we write

$$\frac{\partial}{\partial t} = j\omega_0 + \frac{\partial}{\partial\tau}. \tag{68}$$

Then, in Eq. (67), we can set

$$\frac{\partial^2\phi}{\partial t^2} \approx \omega_0\phi + 2j\omega_0\frac{\partial\phi}{\partial t},$$

$$\frac{\partial\epsilon}{\partial t} = \frac{\partial\epsilon}{\partial\tau}; \qquad \frac{\partial^2\epsilon}{\partial t^2} = 0. \tag{69}$$

With the above simplifications, Eq. (67) reduces to

$$\nabla^2\phi - \omega_0^2\mu_0\epsilon\phi = 2j\omega_0\mu_0\epsilon\frac{\partial\phi}{\partial t} + 2\mu_0\frac{\partial\epsilon}{\partial t}\left[\frac{\partial\phi}{\partial\tau} + j\omega_0\phi\right]$$

$$\approx 2j\omega_0\mu_0\epsilon\left[\frac{\partial\phi}{\partial\tau} + \frac{1}{\epsilon}\frac{\partial\epsilon}{\partial\tau}\phi\right]. \quad (70)$$

Our approach is to develop from Eq. (70) a set of equations to describe the time evolution of the electromagnetic field. We proceed on the basis that a solution ϕ_0 of the stationary wave Eq. (71) is known:

$$\left(\frac{d^2}{dx^2} - \beta_0^2\right)\phi_0 + \epsilon_0 k_0^2\phi_0 = 0. \quad (71)$$

Here β_0 is the z-direction propagation constant, ϵ_0 is the effective dielectric constant for the stationary case, and k_0 is the free-space wave number.

The stationary solution will, in fact, have been obtained within a self-consistency scheme such that it satisfies both Eq. (71) and the stationary diffusion Eq. (72), which is written in a form appropriate to low-doped devices:

$$D\frac{d^2N_0}{dx^2} + \frac{J(x)}{ed} = g_1(x)P_0(x) + BN_0^2, \quad (72)$$

where $N_0(x)$ is the electron density.

Here D is the diffusion coefficient, $J(x)$ is the injected current profile, d is the active region thickness, $g_1(x) = \alpha N_0 - \beta$ is the local gain, $P_0(x)$ is the stationary lasing-field intensity, and B is the coefficient of the bimolecular spontaneous emission rate.

The self-consistency criteria will fix the amplitude A_0 of the lasing field ϕ_0 under stationary conditions. We introduce the notation $\Phi_0 = A_0\phi_0$ and seek a representation of the time-dependent modal field Φ. The time-dependent field is written as a perturbation of Φ_0:

$$\Phi = \Phi_0 + \phi. \quad (73)$$

The perturbation ϕ is expressed as a linear combination of orthogonal functions. It is natural to choose ϕ_0 as one basis function and to construct another basis function ϕ_1 orthogonal to ϕ_0 in a sense defined below in Eq. (75). Using these two functions, we define

$$\phi(x,t) = a_0(t)\phi_0(x) + a_1(t)\phi_1(x), \quad (74)$$

where ϕ_1 is defined such that

$$\int_{-\infty}^{\infty}\phi_1^*(x)\phi_0(x)dx = 0. \quad (75)$$

We point out that in Eq. (74) the coefficients a_0 and a_1 include the time dependence of the perturbation. In general, a_1 is a complex quantity, but a_0 may be taken as a real number. Our attention is now directed at obtaining rate equations for a_0 and a_1.

Inserting Φ from Eq. (73) into Eq. (71) and retaining terms to first order in the perturbation, we obtain

$$\left(\frac{d^2}{dx^2} - \beta_0^2\right)\phi + \epsilon_0 k_0^2\phi - 2j\frac{k_0}{c}\epsilon_0\frac{\partial\phi}{\partial\tau}$$

$$= -\eta k_0^2\Phi_0 + \frac{2jk_0}{c}\frac{\partial\epsilon}{\partial\tau}\Phi_0 + 2\beta_0 b\Phi_0, \quad (76)$$

where $\eta = \epsilon - \epsilon_0$ is the perturbation of the dielectric constant and b is the perturbation of the longitudinal propagation constant β_0.

Further, on introduction of ϕ from Eq. (74) and by using Eq. (71), the wave equation becomes

$$\left(\frac{d^2}{dx^2} - \beta_0^2\right)(a_1\phi_1) + \epsilon_0^2 k_0^2 a_1\phi_1 - 2j\frac{k_0}{0}\epsilon_0(a_0\phi_0 + a_1\phi_1)$$

$$= -\eta k_0^2 A_0\phi_0 + 2j\frac{k_0}{c}\epsilon A_0\phi_0 + 2\beta_0 b A_0\phi_0. \quad (77)$$

To extract rate equations for a_0 and a_1 from Eq. (77), use is made of the orthogonality relation of Eq. (75), and we obtain

$$-2j\frac{k_0}{c}\dot{a}_0\epsilon_{00} - 2j\frac{k_0}{c}\dot{a}_1\epsilon_{01} + a_1\beta_{01}^2$$

$$= +2j\frac{k_0}{c}A_0(\dot{\epsilon})_{00} - k_0^2 A_0\eta_{00} + 2\beta_0 b A_0 \quad (78)$$

and

$$-2j\frac{k_0}{c}\dot{a}_0\epsilon_{10} - 2j\frac{k_0}{c}\dot{a}_1\epsilon_{11} + (\beta_1^2 - \beta_0^2)a_1$$

$$= +2j\frac{k_0}{c}A_0(\dot{\epsilon})_{10} - k_0^2 A_0\eta_{10}, \quad (79)$$

where we have defined

$$\beta_1^2 = \int_{-\infty}^{\infty}\phi_1^*\frac{d^2}{dx^2}\phi_1 dx + \epsilon_{11}k_0^2 \quad (80)$$

and

$$\beta_{01}^2 = \int_{-\infty}^{\infty}\phi_0^*\frac{d^2}{dx^2}\phi_1 dx + \epsilon_{01}k_0^2. \quad (81)$$

The remaining coefficients of Eqs. (78) and (79) are obtained as matrix elements of ϵ, $\dot{\epsilon}$, and η among various combinations of ϕ_i with subscripts indicating which of the basis functions is used. In order to evaluate terms such as $(\dot{\epsilon})_{00}$ appearing in Eqs. (78) and (79), a discussion of the time dependence of the charge-carrier concentration is required. In the next subsection, we turn to this aspect of the problem.

B. Time-Dependent Diffusion Equation

The first-order perturbation of the time-dependent rate equation can be written in the form

$$\frac{\partial n}{\partial t} + \frac{2n}{\tau_s} + \alpha n P_0 = -g_0 P, \quad (82)$$

where

$$P = \Phi_0^*\phi + \phi^*\Phi_0; P_0 = A_0^2|\phi_0|^2 = S_0|\phi_0|^2.$$

Using Eq. (74), we have

$$P = A_0[a_1\phi_1\phi_0^* + a_1^*\phi_1^*\phi_0 + 2a_0|\phi_0|^2]. \quad (83)$$

To describe the time evolution of the electron distribution, we introduce orthonormal functions $\hat{N}_0(x)$ and $\hat{N}_1(x)$. $\hat{N}_0(x)$ is the normalized stationary electron distribution, i.e.,

$$\hat{N}_0(x) = \frac{1}{N}N_0(x), \quad (84)$$

where

$$N = \left[\int_{-\infty}^{\infty} N_0^2(x)\mathrm{d}x\right]^{1/2}. \tag{85}$$

Thus we have

$$\int_{-\infty}^{\infty} \hat{N}_0(x)\hat{N}_0(x)\mathrm{d}x = 1, \tag{86}$$

and $\hat{N}_1(x)$ is defined such that

$$\int_{-\infty}^{\infty} \hat{N}_0(x)\hat{N}_1(x)\mathrm{d}x = 0. \tag{87}$$

With these definitions, we set

$$n(x,t) = \nu_0(t)\hat{N}_0(x) + \nu_1(t)\hat{N}_1(x). \tag{88}$$

This representation of the perturbation of the carrier concentration is introduced into the rate Eq. (82) and leads to rate equations for $\phi_0(t)$ and $\nu_1(t)$. Directly from Eqs. (68) and (80) we obtain

$$\dot{\nu}_0\hat{N}_0 + \dot{\nu}_1\hat{N}_1 = -\frac{2}{t_s}(\nu_0\hat{N}_0 + \nu_1\hat{N}_1) - \alpha P_0(\nu_0\hat{N}_0 + \nu_1\hat{N}_1) - g_0(2A_0a_0|\phi_0|^2 + A_0a_1^*\phi_0\phi_1^* + A_0a_1\phi_0^*\phi_1. \tag{89}$$

Then, by taking advantage of the orthogonality properties of $\hat{N}_0(x)$ and $\hat{N}_1(x)$ as defined by Eqs. (86) and (87), we obtain Eqs. (90) and (91) from Eq. (89)

$$\dot{\nu}_0 = +B_{11}\nu_0 + B_{12}\nu_1 + B_{13}a_0 + B_{14}a'_1 + B_{15}a''_1, \tag{90}$$

$$\dot{\nu}_1 = +B_{21}\nu_0 + B_{22}\nu_1 + B_{23}a_0 + B_{24}a'_1 + B_{25}a''_1, \tag{91}$$

where a single prime indicates a real part and a double prime an imaginary part. The coefficients of Eqs. (90) and (91) are defined in Ref. 21.

We may relate a perturbation n in the electron concentration to a perturbation η in the dielectric constant by means of the expression

$$\eta = (-\rho + j)\frac{\alpha\omega_0 n}{V^2k_0^2}. \tag{92}$$

Here $V = c/n_0$ is the velocity of light in the laser material of refractive index n_0; ρ measures the relative strengths of the gain-guiding and refractive-index antiguiding mechanisms that act on the optical field.

Equation (92) may thus be utilized in conjunction with Eqs. (90) and (91) to obtain expressions for the matrix elements of η and ϵ that appear in Eqs. (78) and (79).

C. Photon Balance

In order to complete the specification of the optical field, it is necessary to discuss the intensity of the field when a perturbation from a stationary state occurs. The perturbed field distribution has already been defined in Eq. (81), and we can thus obtain the perturbation in the field intensity as

$$s = \int_{-\infty}^{\infty} p(x)\mathrm{d}x = 2A_0a_0, \tag{93}$$

where use has been made of the orthogonality of ϕ_0 and ϕ_1^*.

The first-order rate equation for the photon number may be written as

$$\mathrm{d}s/\mathrm{d}t = \delta g S_0 = 2b''VS_0, \tag{94}$$

where b, as discussed previously, is the perturbation in the longitudinal constant and b'' is the imaginary part of b. From Eqs. (90) and (91), we deduce that

$$a_0 = Vb''A_0. \tag{95}$$

Taking b from Eq. (78) leads to the rate equation

$$\dot{a}_0\left(\frac{1}{V} + \frac{\epsilon'_{00}}{cn_0}\right) + \frac{1}{cn_0}\epsilon'_{01}\dot{a}'_1 - \frac{1}{cn_0}\epsilon''_{01}\dot{a}''_1 + \frac{A_0}{cn_0}(\dot{\epsilon})'_{00} = \frac{1}{2n_0k_0}\mathrm{Im}(\beta_{01}^2)a'_1 + \frac{1}{2n_0k_0}\mathrm{Re}(\beta_{01}^2)a''_1 + \frac{k_0}{\epsilon_0n_0}A_0n''_{00}. \tag{96}$$

Equations (79), (90), and (91) provide a full description of the dynamical behavior of the semiconductor laser. The time evolution of the device is specified by rate equations for the parameters ϕ_0, ν_1, a_0, and a_1. We note that the real and imaginary parts of a_1 bring the total number of variables to five. Equations (90), (91), and (96), together with the real and imaginary parts of Eq. (79), represent the required number of rate equations for the variables.

In the next subsection, we wish to collate the rate equations derived in the foregoing analysis and also to complete the introduction of the notation that is convenient for discussion of the Hopf bifurcation algorithm given in Section 3.

D. Matrix Equations of Motion

The preceding analysis has provided linearized rate equations for the variables ν_0, ν_1, a_0, a'_1, and a''_1. The first two variables describe the time evolution of the carrier concentration; the time dependence of the optical field is specified by the remaining parameters. We now wish to introduce a matrix formulation of the foregoing rate equations. Application of the Hopf bifurcation algorithm to the semiconductor laser will then follow in a natural way.

By making the identifications

$$X_1 = \nu_0, \quad X_2 = \nu_1, \quad X_3 = a_0, \quad X_4 = a'_1, \quad X_5 = a''_1,$$

we may write the equations of motion obtained from Eqs. (90), (91), and (96) in the form

$$C\frac{\mathrm{d}X}{\mathrm{d}t} = BX, \tag{97}$$

where B and C are 5×5 matrices whose elements are, in general, complex, and $X^T = [X_1X_2X_3X_4X_5]$.

Provided that C is nonsingular, we thus have

$$\mathrm{d}X/\mathrm{d}t = C^{-1}BX = AX. \tag{98}$$

The elements of matrices B and C are defined in Ref. 21.

The specification of the time evolution of the laser contained in Eq. (98) was the principal aim of the analysis of this section. It is now possible to proceed to a description of the Hopf bifurcation algorithm. It will quickly become apparent that direct application of the algorithm to the semiconductor laser is facilitated by the foregoing analysis.

E. Bifurcation Theory

To apply the techniques of Hopf bifurcation theory, it is required that the laser be described by an autonomous system of ordinary differential equations[22]

$$dX/dt = f(X, S), \tag{99}$$

where X is an n-dimensional vector and s a real parameter. From this system of equations, the Jacobian matrix is formed:

$$A_{ij} = \partial f^i/dx_j. \tag{100}$$

At a stationary point of the system (i.e., under steady-state conditions where $dX/dt = 0$), the eigenvalues of the matrix A are found. The eigenvalues are ordered according to the magnitude of their real parts:

$$\lambda'_1 \geq \lambda'_2 \geq \ldots \geq \lambda'_n. \tag{101}$$

A critical point of the system is identified by finding a value S_c of the bifurcation parameter for which

$$\lambda_1(S) = \lambda^*_2(S) \tag{102}$$

for values of S in the neighborhood of S_c:

$$\left.\frac{d\lambda'_1}{dS}\right|_{S=S_c} \neq 0,$$

$$\lambda''_1(S_c) \neq 0,$$

$$\lambda'_j(S_c) < 0, \qquad j = 2, n.$$

It is now required to apply this algorithm to the dynamics of the semiconductor laser.

It is appropriate also to note here that the formulation of the rate Eqs. (78), (79), (90), and (91) given above has utilized a particular set of basis functions defined in Eqs. (73)–(87). A natural choice of basis functions has been made to relate to the physical problem that underlies the analysis, namely, the occurrence of transverse mode switching in the device. The power of the Hopf bifurcation algorithm becomes apparent when consideration is given to the implications of the choice of an alternative set of basis functions for expansion of the optical field perturbation. With suitable choice of orthogonal functions, it should be practical to study the possibility of a variety of oscillations related to physically occurring optical field perturbations, including those related to longitudinal mode effects.

F. Application to Laser Instabilities

We have already made the identification between the parameters ν_0, ν_1, a', a'', and a five-dimensional vector X. Furthermore, equations of motion have been obtained in the form required by Eq. (99). In deriving the linearized form of the equations as given in Eq. (98), we have, in fact, defined the Jacobian matrix sought by the algorithm. The notation used in Subsection 7.D was deliberately chosen to underline this step. It is clear that the linearization of the laser equations of motion has led naturally to the definition of the matrix whose eigenvalues must be found to follow through the Hopf bifurcation criteria.

At a critical point, the steady-state solution will branch into two oscillatory solutions of the device equations. The ability to identify such points is of value in designing switches and oscillators that make use of the nonlinear properties of semiconductor lasers. Quite apart from temporal instabilities, we are also able to identify discontinuities in the matrix eigenvalues with nonlinearities in the light-current characteristics associated with spatial instabilities under steady-state conditions.

Table 1. Output Power Dependence of λ_1

Output power S (mW)	λ'_1	$\lvert\lambda''_1\rvert$
1.65	3.5×10^{10}	8.8×10^{10}
2.07	3×10^{9}	5×10^{10}
2.8	1.5×10^{8}	3×10^{10}
2.9	-9.1×10^{6}	2.8×10^{10}
3.03	-1.6×10^{8}	2.6×10^{10}

G. Identification of a Critical Point of the System

We consider first a stripe-geometry GaAs laser with an active region thickness d of 0.3 μm and a stripe width of 6 μm. Assumed material parameters are $B = 1.0 \times 10^{-10}$ cm^3/sec (72); $\rho = 2.5(92)$; local gain coefficients $\alpha = 3 \times 10^{-6}$ cm^3/sec; $\beta = 4.5 \times 10^{12}$ sec^{-1}. The photon lifetime in the device is taken as 3 psec.

Calculated values of the leading eigenvalue λ_1 as a function of the Hopf bifurcation parameter—the optical output power per facet—are shown in Table 1. It is deduced from the results shown in the table that a zero of λ'_1 occurs for a value of S of about 2.9 mW. For all the values of S shown above, it is the case that $\lambda_1 = \lambda^*_2$; the absolute value of $|\lambda''_1|$ is included to illustrate that the condition $\lambda'_j < 0$, $j = 3, 4, 5$ holds. Furthermore, in the vicinity of the $S_c = 2.9$ mW, we also have

$$\left.\frac{d\lambda'_1}{ds}\right|_{S=S_c} \neq 0$$

and

$$\lambda''_1(S_c) \neq 0.$$

It is therefore concluded that $S_c = 2.9$ mW is a critical point of the system and, furthermore, that the criteria for the occurrence of a Hopf bifurcation are met at this point. We thus have illustrated the successful application of the Hopf bifurcation algorithm to the analysis of the semiconductor laser.

9. CONCLUSIONS

We have presented an overview of the development of theoretical techniques for the analysis of spatial and temporal instabilities in laser devices. As the family of these devices is growing rapidly and more research emphasis is placed on controlled nonlinearity and instability for optical logic, we expect that new problems will also arise with a concomitant requirement for new theoretical insight.

REFERENCES

1. See, e.g., D. Kerps, "Filament displacement and refraction losses in a stripe-geometry AlGaAs d-h laser," Proc. Inst. Electr. Eng. Part I 127, 94–97 (1980).
2. K. A. Shore and T. E. Rozzi, "Stability analysis of transverse modes in stripe-geometry injection lasers," Proc. Inst. Electr. Eng. Part I 128, 154–159 (1981).

3. K. A. Shore and T. E. Rozzi, "Near field control in multi-stripe geometry injection lasers," IEEE J. Quantum Electron. **QE-17**, 718–722 (1981).
4. K. A. Shore, T. E. Rozzi, and G. in't Veld, "Semiconductor laser analysis: a general method for characterizing devices of various cross-sectional geometries," Proc. Inst. Electr. Eng. Part I **127**, 221–229 (1980).
5. J. Katz, "Electronic beam steering of semiconductor injection lasers: a theoretical analysis," Appl. Opt. **22**, 313–317 (1983).
6. K. A. Shore and P. J. Hartnett, "Diffusion and waveguiding effects in twin-stripe injection lasers," Opt. Quantum Electron. **14**, 169–176 (1982).
7. K. A. Shore, "Above threshold current leakage effects in stripe-geometry injection lasers," Opt. Quantum Electron. **15**, 371–379 (1983).
8. K. A. Shore, N. G. Davies, and K. Hunt, "Constant power contours and bistability in twin-stripe injection lasers," Opt. Quantum Electron. **15**, 547–548 (1983).
9. I. H. White, J. E. Carroll, and R. G. Plumb, "Closely coupled twin-stripe lasers," Proc. Inst. Electr. Eng. Part I **129**, 291–296 (1982).
10. D. R. Scifres, W. Streifer, and R. D. Burnham, "Beam scanning with twin stripe injection lasers," Appl. Phys. Lett. **33**, 702–704 (1978).
11. K. A. Shore, "Optically induced spatial instability in twin-stripe geometry lasers," Opt. Quantum Electron. **14**, 177–181 (1982).
12. K. A. Shore, "Near field extinction in semiconductor lasers under optical injection," Opt. Quantum Electron. **16**, 157–164 (1984).
13. K. A. Shore, "Semiconductor laser bistable operation with an adjustable trigger," Opt. Quantum Electron. **14**, 321–326 (1982).
14. K. A. Shore, "Optical limiter action in twin-stripe geometry lasers," Proc. Inst. Electr. Eng. Part I **129**, 297–300 (1982).
15. K. A. Shore, "Radiation patterns for optically steered semiconductor laser beam-scanner," Appl. Opt. **23**, 1386–1390 (1984).
16. K. A. Shore and T. E. Rozzi, "Switching frequency for transverse modes in stripe-geometry injection lasers," Opt. Quantum Electron. **15**, 497–506 (1983).
17. K. A. Shore and T. E. Rozzi, "Transverse mode oscillations at GHz frequencies in stripe-geometry lasers," Opt. Quantum Electron. **14**, 465–466 (1982).
18. K. A. Shore and T. E. Rozzi, "Picosecond optical switching in semiconductor lasers," Opt. Quantum Electron **15**, 549–552 (1983).
19. B. S. Poh, T. E. Rozzi, and C. H. Velzel, "Single- and dual-filament self-sustained oscillations in *dh* injection lasers," Proc. Inst. Electr. Eng. Part I **126**, 233–241 (1979).
20. B. S. Poh and T. E. Rozzi, "Intrinsic instabilities in narrow stripe geometry lasers caused by lateral current spreading," IEEE J. Quantum Electron. **QE-17**, 723–731 (1981).
21. K. A. Shore and T. E. Rozzi, "Transverse switching due to Hopf bifurcation in semiconductor lasers," IEEE J. Quantum Electron. **QE-20**, 246–255 (1984).
22. B. D. Hassard, N. D. Kararinoff, and Y. H. Wau, *Theory and Applications of Hopf Bifurcation* (Cambridge U. Press, London, 1981).

T. E. Rozzi

T. E. Rozzi obtained the degree of *dottore* in physics from the University of Pisa in 1965 and the Ph.D. degree in Electronic Engineering from Leeds University in 1968. From 1968 to 1978, he was a research scientist at the Philips Research Laboratories, Eindhoven, The Netherlands, having spent one year (1975) at the Antenna Laboratory, University of Illinois, Urbana, Illinois. In 1978, he was appointed to a chair of electrical engineering at the University of Liverpool; he was subsequently appointed to a chair of electronics and head of the Electronics Group at the University of Bath in 1981. He is currently head of the School of Electrical Engineering, University of Bath, Bath, UK. In 1975, he was awarded the Microwave Prize of the Microwave Theory and Techniques Group of the Institute of Electrical and Electronics Engineers.

K. A. Shore

K. A. Shore was born on June 11, 1950, in New Tredegar, Wales. He received the B.A. degree in mathematics from Oxford University, England, in 1971 and the Ph.D. degree in applied mathematics from University College, Cardiff, Wales, in 1975. His thesis was concerned with a self-consistent computer model of the double-heterostructure laser. He spent a year as a postdoctoral research assistant at the Department of Applied Physics and Electronics, UWIST, Cardiff, Wales, before moving to the Department of Computing there. In 1979, he was appointed lecturer in the Department of Electrical Engineering and Electronics, University of Liverpool, England. Since October 1983, he has been a lecturer in the School of Electrical Engineering, University of Bath, Bath, UK. His recent research has concerned the characterization of multistripe geometry lasers and the stability properties of lasers, with particular reference to optical bistability and switching.